# Projection x-ray lithography implemented using point sources

I. A. Artyukov, L. L. Balakireva, F. Bijkerk,[1)] A. V. Vinogradov, N. N. Zorev, I. V. Kozhevnikov, V. V. Kondratenko,[2)] O. F. Ogurtsov,[3)] A. G. Ponomarenko,[2)] and A. I. Fedorenko[2)]

*P. N. Lebedev Physics Institute, Academy of Sciences of the USSR, Moscow;*
*Laser Application and Information Centre, Amsterdam, Nieuwegein, Netherlands;*
*V. I. Lenin Polytechnic Institute, Kharkov;*
*Scientific-Research Institute of Molecular Electronics, Zelenograd*
(Submitted June 20, 1991)
Kvantovaya Elektron. (Moscow) **19**, 114–127 (February 1992)

An analysis is made of the state of the art of x-ray lithography and x-ray optics. The principles of design and configurations of projection x-ray lithographic systems are considered. An analysis is made of the main trends of research on these topics proceeding in the laboratories in the Soviet Union, USA, Japan, and Great Britain. The problems encountered in the development of multilayer normal-incidence x-ray mirrors are described.

**CONTENTS**



## INTRODUCTION

The progress in microelectronics industry is indissolubly related to the progress in microminiaturization, which makes it possible to form over $10^6$ components in one integrated-circuit chip. Reduction in the size of electronic components can be demonstrated by the following examples. In 1960 a board of $10\times 12$ cm dimensions carried 3–4 logic circuits, whereas now hundreds of thousands of such circuits are carried by a chip whose area is a few square millimeters.[1] Since 1970 the number of components in one integrated-circuit chip has increased by a large factor and it is forecast to approach $10^9$ per crystal by the year 2000. This reduction in the dimensions of transistor components has greatly reduced the response time of the electronic circuits and the cost of calculations (Fig. 1).[2] These factors are among the causes of the boom called modern industrial revolution.

The key stage in the manufacture of microelectronic integrated circuits is lithography. Modern lithography represents a number of stages and technological processes, which are related in a complex manner:[3]

1) exposure equipment determines the resolution, the precision of register, and the cost;

2) the resists govern the productivity and quality of the images;

3) development of the resist determines the tolerances and quality of the images;

4) etching or explosive lithography governs the tolerances and quality of the images;

5) metrology provides the monitoring of the parameters;

6) control of contamination influences the yield of acceptable components.

In the modern mass production of integrated circuits the major cost of lithographic equipment is that of the optical exposure apparatus. An increase in the degree of integration of microcircuits is setting increasingly stringent requirements in respect of the resolution, which must be ensured reliably during exposure (Fig. 2). An additional stimulus for the development of lithographic exposure systems capable of submicron resolution will be provided by the appearance of ultrafast microelectronics based on high-temperature superconductors, which will make use of conventional superconductor components (Josephson junctions) with characteristic dimensions of $\sim 0.01$ $\mu$m, as well as hybrid semiconductor–superconductor circuits.[5,6]

Obviously, the resolution $\delta_d$ in the exposure stage is limited by the diffraction of the radiation used to illuminate a resist. The resolution of an objective, determined for two opaque objects which are barely distinguishable in an Airy

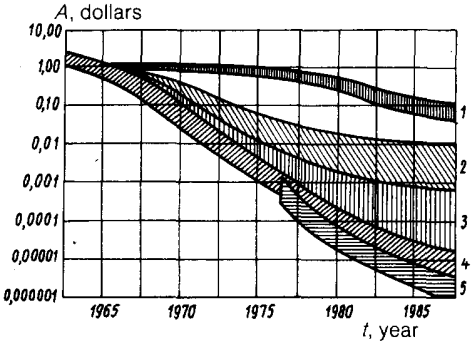


FIG. 1. Reduction of the cost, by microminiaturization, of one function $A$ performed by different types of integrated circuits (Ref. 2): *1*) conventional integrated circuits; *2*) hybrid circuits; *3*) bipolar circuits; *4*) metal–oxide–semiconductor structures; *5*) submicron circuits.

 0049-1748/92/020099-12$06.00  

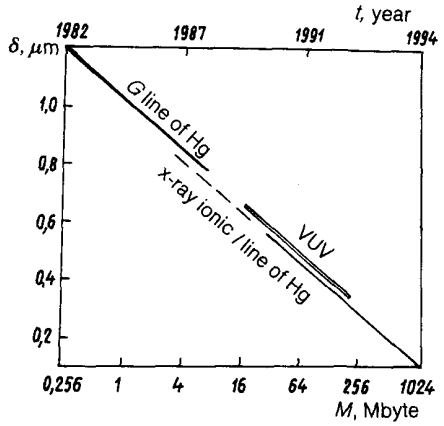


FIG. 2. World trends in the design of lithographic equipment[4] ($\delta$ is the resolution and $M$ is the capacity of memories).

disk, is determined by the Rayleigh criterion:

$$\delta_d = k\lambda/N_a, \tag{1}$$

where $\lambda$ is the wavelength of the radiation used in the exposure process and $N_a$ is the numerical aperture of the objective. The coefficient $k \geqslant 0.3$ applies to resists forming an image in the upper surface layer, $k \geqslant 0.5$ applies to multilayer resists, whereas $k \geqslant 0.75$ and $k \geqslant 1.1$ are typical of single-layer resists and those deposited on reflecting surfaces.[7] It is clear from Eq. (1) that the resolution improves when we use radiation of shorter wavelengths and optics with a larger aperture.

Unfortunately, an increase in the numerical aperture $N_a$ reduces strongly the depth at which the image is sharp

$$DF = \pm\lambda/2N_a^2, \tag{2}$$

increases the complexity of the optical components, and makes them more expensive. For these reasons, extensive use of optical exposure systems characterized by $N_a > 0.3$–$0.4$ is unlikely.

It therefore follows that progress in modern submicron lithography will require development of methods for exposure using radiation of wavelengths $\lambda < 10$ nm (Table I, Fig. 2). Moreover, the use of high-energy x-ray radiation for exposure purposes will minimize the influence of small particles on the image quality. It is known that particles of $d < 0.5$ $\mu$m dimensions are a major problem in submicron photolithography because of the high sensitivity of this technology to submicron contamination of the template and resist (Fig. 3). In the case of x-ray radiation, such particles (with the exception of those made of heavy elements) are transparent because of their weak x-ray absorption. This reduces greatly the number of defects in integrated circuits and makes it possible to relax the conditions that must be satisfied in the

TABLE I. High-resolution lithography.[3]

| Radiation | Energy, keV | $\lambda$, nm |
|---|---|---|
| Electron beam | 2–100 | 0.1 |
| Ion beam | 10–300 | 0.1–0.5 |
| X-ray irradiation | 0.15–3 | 0.4–10 |

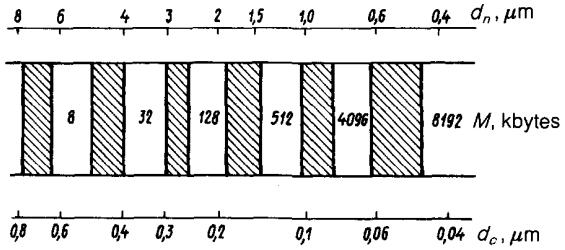


FIG. 3. Normal minimum ($d_n$) and critical ($d_c$) dimensions of defects or particles in memories.[8]

extensive "clean rooms" where fabrication takes place.

A comparison of the attractions and competitiveness of the various methods for submicron radiation lithography of integrated circuits (utilizing electron beams, ion beams, or x-ray radiation) leads to the conclusion that x-ray radiation is preferable for the following reasons. X-ray lithography is characterized by a higher productivity than lithography by electron or ion beams and, consequently, the intrinsic cost of integrated circuits is then lower. An important advantage is the absence of the proximity effect, caused by the backscattering of electrons, typical of electron-beam lithography. This makes it possible to use relatively thick resist films in x-ray lithography. Finally, as mentioned already, the problem of surface contamination of the template and resist is much less acute in x-ray lithography.

However, in spite of very optimistic forecasts (see, for example, Ref. 4) the adoption of the new technology of manufacture of submicron integrated circuits based on x-ray exposure has raised the problem of x-ray radiation sources which do not yet satisfy the requirements of mass manufacture of integrated circuits, because the available sources are expensive and suffer from low intensities and a short service life.

## 1. X-RAY SOURCES USED IN LITHOGRAPHY

The work on the equipment needed in x-ray lithography has been proceeding along two directions: the development of compact synchrotron sources with systems to ensure coincidence and replication (steppers) and the development of x-ray lithographic equipment with point x-ray sources.

Synchrotron sources have a number of advantages, which is the reason for the intense work in various establishments, scientific centers, and organizations on the development and use of synchrotron sources in microelectronics.[9,10] The main advantages of synchrotron radiation are its small angular divergence and high intensity (100–200 mW/cm$^2$ on the surface of a plate), which ensure that high-quality images can be formed and the x-ray lithographic productivity is high. The latest report from Japan describes an ultracompact Aurora storage ring with a diameter of 1 m. This ring is fitted with 16 steppers.[11]

However, in view of the high cost of construction of a synchrotron facility (which exceeds 100 million rubles) and of its operation, facilities of this type can be used effectively only in large scientific–technical centers. Moreover, the use of a synchrotron as a radiation source in industry is hardly justified because in this case the industrial process of microcircuit fabrication will be governed entirely by the period of failure-free operation of just one component of a very com-

TABLE II. X-ray sources.

| Laboratory, organization | Country | Type of source | Wavelength, nm | Size of source, mm | Output power or energy | General description of class of sources |
|---|---|---|---|---|---|---|
| Hewlett–Packard | USA | electron–beam | 0.44 | 1.5 | 34 $\mu$W/sr | total cost 100–200 thousand dollars, used probably up to 1989, intensity up to 1 mW/cm$^2$, efficiency ~0.01%, source size several millimeters |
| NTT | Japan | electron–beam | 0.71 | 3 | 1 mW/cm$^2$ | |
| Micronix | USA | electron–beam | 0.44 | 3.5 | | |
| Perkin–Elmer | USA | electron–beam | 0.70 | 1.5 | | |
| SRIME | USSR | electron–beam | 1.33 | 3 | 0.1 mW/cm$^2$ | |
| Micronix | USA | plasma | | | | total cost 350–400 thousand dollars, intensity to ~10 mW/cm$^2$ source size 0.1–1.0 mm, efficiency 0.15–3.7% |
| Physics Intern. Pixi | USA | plasma pinch | 0.7 | | 250 J/pulse (1 Hz) | |
| Karl Suss LSX-10 | Germany | plasma | 0.7–1.2 | | 250 J/pulse (1 Hz) | |
| Perkin–Elmer and Maxwell Industries | USA | plasma pinch | 0.74 | | 15 mW/cm$^2$ (10 Hz) | |
| NTT | Japan | plasma | 0.9–1.4 | 1 | 10 mW/cm$^2$ | |
| Hitachi | Japan | plasma focus | | | 100 J/pulse | |
| SRIME, FIAS | USSR | plasma pinch | 1–2 | 1.0 | 10 J/pulse (5 Hz) | |
| Rochester University and Exxon Research | USA | laser-plasma (neodymium laser) | | 0.1 | 35 J/pulse | intensity in excess of 10 mW/cm$^2$, source size less than 0.1 mm, efficiency 10% |
| Varian Associates | USA | laser-plasma | | 0.1 | 20 mW/cm$^2$ | |
| Osaka City University | Japan | laser-plasma | | hollow gold target | | |
| Rutherford Laboratory | England | laser-plasma (excimer laser) | | | | |
| IAE | USSR | laser-plasma (excimer laser | 1–2<br>0.5–1.5 | 0.1 | 10 J/pulse (10–20 Hz) | |
| AUSTRIPTREM | USSR | laser-plasma (neodymium laser) | 1–2 | 0.1 | 10 J/pulse | |

*Note.* Soviet research institutes: SRIME is the Scientific-Research Institute of Molecular Electronics; FIAS is the Physics Institute, Academy of Sciences of the USSR; IAE is Institute of Atomic Energy; AUSRIPTREM is All-Union Scientific-Research Institute of Physicotechnical and Radio Engineering Measurements.

plex facility and that component is the synchrotron. Therefore, the development designed to construct alternative sources of x-ray radiation, which would make it possible to use x-ray lithography in industry, is exceptionally important and urgent. These are point sources of x rays being developed by many organizations and enterprises. Tables II and III show at a glance the trends in the development of x-ray lithographic equipment and point sources. We can see that the development of such sources occurred in three stages. These stages or generations are characterized by specific

TABLE III. X-ray lithographic equipment.

| Maker, model | Country | Source | $\lambda$, nm | Minimum size, $\mu$m | Precision of register, $\mu$m | Productivity, boards/h | Ref. |
|---|---|---|---|---|---|---|---|
| NTT SR-1 | Japan | electron-beam | 0.71 | 0.5 | 0.1 | | 15 |
| TCSF XPWS 301 | USA | electron-beam | 1.33 | 0.2 | 0.05 | | 15 |
| SRIME KBTÉM | USSR | electron-beam | 1.33 | 0.5 | 0.15 | 2 | |
| Bell Labs. Micronix | USA | electron-beam | 0.44 | 0.5 | 0.1 | 10 | 15 |
| Perkin–Elmer XLS-1000 | USA | electron-beam | 0.7 | 0.5 | 0.1 | 10 | 16 |
| Nikon SX-5 | Japan | electron-beam | 0.71 | 0.5 | 0.1 | 6 | 17 |
| NTT (modernized SR-1) | Japan | plasma | 0.9–1.4 | 0.5 | 0.05 | 20 | 18 |
| Karl Suss XRS-200, LSX-10 | Germany | plasma | 0.7–1.2 | | 0.05 | | 17 |
| Hampshire Instruments XRL-5000 | USA | laser-plasma | | 0.25 | 0.1 | 25–50 | 12 |
| Matsushita Electrical Industries (MEI) | Japan | laser-plasma | | 0.2 | | | 13 |

*Note.* Here, SRIME KBTÉM represents KBTÉM system developed at the Scientific-Research Institute of Molecular Electronics.

types of x-ray sources which in the final analysis determine the resolution and productivity of x-ray lithographic equipment.

The first generation is represented by electron-beam sources with a resolution of $\sim 0.5\,\mu$m, the second are plasma sources with a resolution $\sim 0.5$–$0.3\,\mu$m, and the third are laser-plasma sources with a resolution better than 0.3–0.2 $\mu$m. The resolution of the equipment is determined primarily by the dimensions of the source, which influence the smearing of the image edges. Productivity is governed by the efficiency of the sources and also by the distance from the source to the resist, which in turn affects the resolution.

We shall describe more fully the capabilities of third-generation equipment by considering the XRL-5000 unit made in the USA. The source is a solid-state laser, the x-ray radiation flux density is 10–20 mW/cm$^2$ in the wavelength range 0.8–2.0 nm, and the peak for this flux is at 1.4 nm (Ref. 12). The resolution and productivity of the unit are 0.25 $\mu$m and 25 boards/h, respectively. Similar apparatus was constructed in Japan in 1989 by Matsushita Electrical Industries (MEI).[13]

There is considerable interest in the development of x-ray sources utilizing excimer lasers, which will make it possible to construct high-power sources. An example is the recently developed (at the Sandia National Laboratory, USA) source of soft x-ray radiation.[14] A KrF laser operating at a pulse repetition frequency 100 Hz and with an energy of 1.5 J/pulse made it possible to reach a flux density of 2.2 mW/cm$^2$ (with the peak value $8.3\times 10^2$ W/cm$^2$) at $\lambda = 12.4$ nm ($\Delta\lambda/\lambda \sim 1.6\%$).

## 2. SHADOW X-RAY LITHOGRAPHY USING POINT SOURCES

Experiments on x-ray lithography began about 20 years ago,[19] but the first reports of commercial apparatus appeared only in the last few years and it must be stressed that these are still prototypes. In spite of the very optimistic forecasts mentioned above, x-ray lithography is not yet used widely in industry. One of the main reasons is the insufficiently high power of the point x-ray sources.

We shall illustrate this by considering the example of x-ray tubes. Before discussing the energy parameters, we shall first deal with the spatial resolution problem. All the equipment discussed in the preceding section is intended for contact lithography with a gap (Fig. 4). The obvious requirement in this case is that the scattering spot associated with the half-shadow and diffraction does not exceed a certain size set by the resolution, for example, $s < 0.2\delta$, where $\delta$ is the required minimum size of a component in a crystal. This leads to the following conditions:

$$L > 5ah/\delta, \tag{3}$$

$$\lambda < 0{,}61\delta^2/5h, \tag{4}$$

where $h$ is the gap between the template and the resist (which usually amounts to 20–40 $\mu$m). The conditions (3) and (4) determine the minimum distance from the source to the resist and the maximum wavelength.

According to the estimates of Ref. 20 the modern x-ray tubes ensure [when the condition of Eq. (3) is obeyed] an x-ray flux density not exceeding $10^{-3}$ W/cm$^2$ on the resist surface. In the case of chip-by-chip exposure if the sensitivity of the resist is $\sim 0.1$ J/cm$^2$, this means that one chip requires an exposure of 100 s and one board (with $\sim 100$ chips) needs $10^4$ s $\approx 3$ h. The lowest productivity acceptable in industry is 30 boards/h, i.e., the required productivity is at least 100 times higher than that possible using these sources, so that the forecasts in respect of x-ray tubes should be regarded as overoptimistic. (These requirements are somewhat more relaxed in the case of laser plasma and pinch.)

Consequently, a drastic increase in the power of the sources or of the efficiency of their utilization is required. Let us return back to x-ray tubes. We shall begin now from the total power of the radiation emitted by such a tube within a solid angle $\sim 2\pi$, which is $P_0 \sim 1$ W. A flux (power) density can be created on the surface of a resist so as to ensure that the industrial type of exposure ($q_0 \sim 0.1$ W/cm$^2$) can be achieved collecting at least one-tenth of all the output power on the surface of a chip of $1\times 1$ cm dimensions.

It therefore follows that the problem is the development of a point source with a diameter $\sim 10^2 - 3\times 10^3\,\mu$m and capable of delivering the highest possible flux density to an area of $1\times 1$ cm dimensions; moreover, near the target surface the divergence of the beam should be fairly small ($\alpha = 3\times 10^{-3}$) so as to avoid distortions in the shadow exposure method. If there are no optical components between the source and the resist, then the last requirement means that we have to place a chip at a distance of $L \sim 50$–$100$ cm from the source, which gives the flux density on a resist amounting to $q \approx P_0/4\pi L^2$. Hence, it is clear that the x-ray radiation power reaching the crystal $P \approx qs_0 \approx s_0 P_0/4\pi L^2$ represents only $(1\text{–}3)\times 10^{-5}$ of the total power of the source. We are then faced with a natural question: is it possible to increase this fraction by x-ray optics.

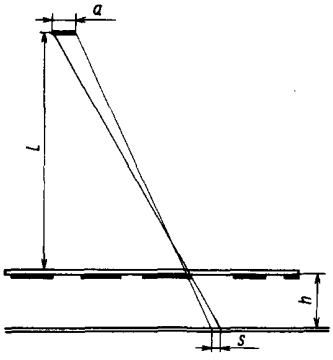


FIG. 4. Schematic diagram showing shadow exposure.

## 3. X-RAY OPTICAL COMPONENTS

The following types of x-ray optical components are known: grazing-incidence optics with one reflection, grazing-incidence optics with multiple reflections (using mirrors for the whispering modes), multilayer normal-incidence optics, diffraction components (zone plates), Bragg–Fresnel optics, and x-ray waveguides. In x-ray lithographic applications the first three types of optical components are the important ones.

1. The traditional grazing-incidence optics is used in x-ray apparatus and in synchrotrons, as well as in microscopes and telescopes, usually employing the Kirkpatrick–Baez or Wolter configurations. If we define the efficiency $\nu$ of the optics as the fraction of the radiation transmitted from a

point source to the surface of a chip, then in the case of the grazing-incidence optics with one reflection the order of magnitude of the efficiency is $\nu \sim \theta_c^2 \approx |1-\varepsilon|$ ($\theta_c$ is the critical angle) i.e., it falls rapidly at short wavelengths. On the other hand, if the optics is used, the efficiency is generally independent of the distance $L$ between the source and chip. The relationship between the maximum efficiency of the grazing-incidence optics and the optical constants of the reflecting coating [$\beta = \mathrm{Re}(1-\varepsilon)$, $\gamma = \mathrm{Im}\varepsilon$] is considered in greater detail in Refs. 21 and 22. The results of Ref. 22 can be used in preliminary estimates, whether it is desirable to use an x-ray concentrator in contact x-ray lithography and also in selection of the reflecting coating. For example, in the $\lambda \approx 4.4$ nm range the use of a nickel reflector makes it possible to collimate up to 2% of the radiation power (in the 0.8–1.2 nm range the efficiency of a rhuthenium reflector is $\nu = 0.2\%$) arriving from a point source. Actual figures may be considerably less because of the need to ensure a uniform illumination of a chip and a specific angular divergence of the radiation [see Eq. (3)]. The final answer to the question of the effectiveness of utilization of an x-ray concentrator in contact lithography can be provided by numerical modeling of the ray paths (see Sec. 6).

It should be pointed out that the use of concentrators of radiation for other purposes (for example, optical pumping of x-ray lasers) was considered in Refs. 22 and 23. The requirements are then less stringent, because there is no need to ensure a certain angular divergence of the pump radiation in the active medium. We are not aware of any experimental work on the use of x-ray concentrators in contact lithography and optical pumping of x-ray lasers.

2. When grazing-incidence whispering-mode mirrors are used, a ray reflected from the mirror returns to it at an angle less than the critical value. In this way an x-ray beam is distributed along the reflecting surface and seems to form an envelope around it. Calculations and measurements have shown[24–27] that whispering-mode mirrors with a suitably selected material of the reflecting coating can rotate beams by angles $\psi = \pi/2$ with an efficiency 20–80% throughout the soft x-ray range. It is shown in Ref. 28 that whispering-mode mirrors can be utilized not only in rotation of narrow parallel beams, but also in collimation of radiation of point sources.

A suitable reflector has the shape of a logarithmic spiral and is an x-ray variant of ideal optical concentrators used in solar energy conversion.[29] Multiple reflections by ideal concentrators play a fundamental role. Only such reflections can ensure the maximum efficiency (amounting to about 100% in the visible range) of transmission of radiation from extended sources to objects. In a spiral x-ray collimator the losses are entirely due to the absorption of radiation in the reflecting coating. The efficiency of such a collimator is

$$\nu = [1+\exp(-\xi\pi)]/2(2+\xi^2),\ \xi = 2\mathrm{Im}(1-\varepsilon)^{-1/2}. \quad (5)$$

Equation (5) gives only the ultimate capability of grazing-incidence reflecting optics. It can be used as the starting point in the selection of the material and shape of the reflector. More realistic values are obtained when x-ray concentrators are modeled by the method of ray tracing.

3. Recent years have seen particularly rapid progress in the development of multilayer x-ray mirrors. They have a number of important advantages over grazing-incidence optics. First of all, they are spectrally selective, which is due to the interference nature of the reflection process. The width of the band where the reflection coefficient differs from zero is of the order of $\Delta\lambda/\lambda \sim \theta_c^2$, but it may be varied by suitable selection of the materials and by altering the ratio of the layer thicknesses; typical values are $\Delta\lambda/\lambda \sim 10^{-1}$–$10^{-3}$. In contrast to the grazing-incidence optics, a multilayer mirror can operate also under normal-incidence conditions. In this case the multilayer coating period is related to the wavelength by the Bragg condition:

$$2d = n\lambda, \quad (6)$$

where $n$ is the diffraction order. Since the thickness of a material layer cannot be less than several atomic radii, it is clear that the condition (6) determines the minimum wavelength at which multilayer optics can be used. However, an even more stringent condition is set by the optical quality of the reflecting coating:

$$\sigma \leqslant \lambda/20, \quad (7)$$

where $\sigma$ is the height of the surface microirregularities. If the condition (7) is disobeyed, then the major part of the radiation is not carried by the specular component, but is concentrated in the diffuse scattering. At present the condition (7) limits the range of applications of normal-incidence multilayer optics to wavelengths of 6–4 nm.

Multilayer mirrors are used widely in many cases because they are easy to make, "flexible," and often less expensive than grazing-incidence mirrors. Variation of the period of the structure, the grazing angle, the composition of the layers and their thickness, makes it possible to impart specific properties of a multilayer mirror. A multilayer coating deposited on a spherical substrate has focusing properties. It can be used as a radiation concentrator and also in image formation. It is the latter that has made it possible to consider the possibility of developing projection x-ray lithography, i.e., the transfer of a pattern from a template to a resist by an x-ray optical system.

## 4. PROJECTION X-RAY LITHOGRAPHY

Investigations of contact (with a gap) x-ray lithography in the last decade or two[20] have revealed a number of shortcomings of such lithography, which hinder greatly its rapid adoption by industry. These shortcomings include above all the low efficiency of utilization of the energy of a point radiation source ($\nu \sim 10^{-4}$–$10^{-5}$) and the problem of a template, related to its high cost, small thickness, and high sensitivity to thermal and mechanical loads. Moreover, the spatial resolution of this method is limited to $\sim 0.3$–$0.3\ \mu$m and a further increase in the degree of integration as well as a possible use of other components (high-temperature superconducting electronics, single-electron electronics, etc.) have made it necessary to search for other lithography methods. Although the use of x-ray concentrators may solve the problem of a radiation source, the other problems are difficult to resolve because of the inflexibility of contact lithography.

Projection x-ray lithography largely avoids these problems[32] and particularly the problem of a template, which can be made reflecting (i.e., massive) or thicker (because of the greater depth of sharpness in the region of an object) and

spatially separate from a resist. Moreover, this lithography makes it possible to extend the range of applications to the spatial resolution $\delta \sim 0.01$–$0.1\ \mu$m.

The selection of the type of the optical components for projection x-ray lithography is determined by the requirements of high energy efficiency and spatial resolution. Although grazing-incidence systems of the Wolter type can, in principle, ensure a high spatial resolution, they require an exceptionally high precision of fabrication and alignment of the components. The precision in their fabrication achieved so far makes it possible to reach resolutions in the range $\delta \sim 1\ \mu$m, whereas attainment of $\delta \sim 0.1\ \mu$m is a difficult technological task.[24] The small numerical aperture and the low efficiency of the diffraction optics also makes it difficult to use it in projection lithography. Grazing-incidence whispering-mode systems considered as radiation concentrators are, in principle, highly efficient, but an image cannot then be obtained at all. Therefore, the most promising are multilayer x-ray mirrors.[33]

In the simplest multilayer system there is only one focusing mirror (Fig. 5), as described in Ref. 30. Calculations show that the configuration in Fig. 5 makes it possible to reach a high spatial resolution ($\delta = 0.01$–$0.03\ \mu$m) and admits the use of an efficient concentrator ($\nu \sim 1$–$20\%$). However, two problems are encountered in this configuration: it is necessary to place a coincidence stage or table in such a way as not to interrupt the rays and a sufficient field of view (based on the chip size) must be ensured. The first task can be performed by cutting a plate into long strips 1 cm wide (of chip size). These strips can be located one behind the other and can be scanned only in a plane parallel to the axis or they can be placed on a tooth-like cassette (Fig. 5) of a stepper, whose plane is parallel to the extreme ray $AB$ from the template to the focusing mirror. The whole lithographic cycle then occurs in the usual way, but a plate is replaced by a cassette with fixed exposed strips. One cassette can carry any number of strips and the number is limited only by technological and cost factors.

The solution of the second task is governed by the need to ensure the necessary spatial resolution. For example, if a spherical surface is used as a focusing mirror, the resolution is given by

$$\delta = C[\varkappa K \lambda^2 H/(1-1/M^2)]^{1/3}, \qquad (8)$$

where $C$ is a coefficient governed by the shape and dimensions of the mirrors; $\lambda$ is the wavelength; $M$ is the reduction coefficient ($M > 1$); $H$ is the linear size of the field of view in the image plane; $\varkappa = \delta_d/\delta_g$ is the ratio of the diffraction resolution to the geometric one; $K$ is the ratio of the geometric resolution, measured at some intensity, to the total size of the scattering circle (defined by the outer rays). It follows from Eq. (8) that the size of the field of view depends very strongly on $\delta$, so that it is possible to reduce greatly the size of the resolved objects only by a strong reduction of the field of view. The value of $\delta$ is minimal for the diameters and radii of curvature of a mirror. For example, if $H = 1$ cm we have $\delta = 0.3\ \mu$m ($M = 10 - \infty$, $\lambda = 4.4$ nm, $\varkappa = 1$, $K = 0.5$). Calculations carried out using the ray tracing program (Sec. 6) show that the correct selection of the mirror parameters can reduce $K$ to $\sim 0.1$–$0.2$, but this increases slightly the value of $C$, so that in practice a spherical mirror can be used for the exposure of a chip of $1 \times 1$ cm size only in the range $\delta \geqslant 0.3\ \mu$m (if $M \gg 1$).

The best resolution in such a field of view can be achieved using either nonspherical mirrors or multicomponent focusing systems. The simplest two-component system is one composed of two spherical mirrors. Successive reflection from these mirrors (which are concave and convex) makes it possible to minimize the spherical aberration and coma while retaining relatively large apertures and fields of view.

An example of such an optical system is the Schwarzschild objective (Fig. 6) used in x-ray microscopy (a variant of a similar optical system used in x-ray projection lithography is the Cassegrain objective[32]). The advantages described above and the simplicity of the optical system have made it popular in a number of designs used in x-ray projection lithography in the USA and Japan. For example, the Schwarzschild objective, composed of multilayer W–C mirrors, had been used to form a structure $0.5\ \mu$m thick in an experiment at a wavelength of 12.4 nm with a fivefold reduction of the size of the reflecting mask.[31]

The main shortcomings of systems of the Schwarzschild type is the high precision needed in setting the mirrors in the longitudinal ($\sim 0.1\ \mu$m) and transverse ($\sim 1'$) directions, as well as the need to allow for the strong distortion. The shortcomings of the Schwarzschild objective have stimulated a search for other two-component systems more suitable for projection x-ray lithography. It may be that optical systems optimal for different ranges of $\delta$ will be developed.

The trend to ensure the minimum diffraction-limit resolution has determined the selection of the minimum permissible (by the multilayer optics) wavelength for projection systems. At present this is $\lambda_{min} = 4$ nm. The reflection coefficient reached in practice is relatively low ($R \sim 10\%$), compared with the theoretical limit $R = 40$–$60\%$, so that each reflecting surface reduces the productivity of a litho-

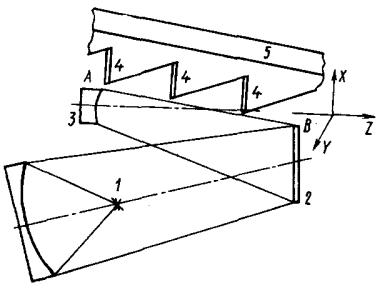


FIG. 5. Projection x-ray lithography with one mirror: *1*) x-ray source; *2*) reflecting template; *3*) imaging mirror with a multilayer coating; *4*) plates carrying a resist; *5*) stepped cassette.

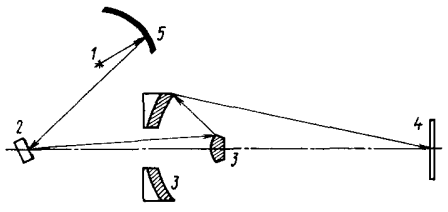


FIG. 6. Schwarzschild objective: *1*) source; *2*) reflecting template; *3*) multilayer spherical mirrors; *4*) plate; *5*) condenser mirror.

graphic system by an order of magnitude. This makes it necessary to optimize first of all the systems in which use is made of a single-component focusing objective.

The search must not be limited to the x-ray optical systems described in the literature and one of the important current tasks in projection x-ray lithography is to find an optimal system. It therefore follows that projection x-ray lithography provides an opportunity of achieving a high resolution and, consequently, a high degree of integration in combination with efficient utilization of radiation from an x-ray source, which eases greatly the task of making and using a template. Moreover, the increase of the wavelength from $\lambda = 0.8$–$1.2$ nm (in contact lithography) to $\lambda \sim 4.4$ nm should increase by almost one order of magnitude the sensitivity of resists and to relax requirements in respect of the radiation source. This justifies the work expended in looking for the solution to the problem in question.

## 5. MULTILAYER X-RAY MIRRORS

In this section we shall discuss two problems in modern multilayer x-ray optics, which are of fundamental importance for the development of projection x-ray lithography. One is the fabrication of short-period normal-incidence mirrors for the range of wavelengths $\lambda < 4.4$ nm and the other is an increase in the time and radiation stability of the mirrors, which is an essential precondition for the use of multilayer optics in mass manufacture of microcircuits. Since there is little information on these problems in current literature on multilayer x-ray optics, we shall consider them in greater detail. Both problems are important not only in the case of point sources, but perhaps even to a greater extent when synchrotron radiation is used.

Theoretical calculations show that at any wavelength in the soft x-ray range it is possible, in principle, to make multilayer mirrors with the normal-incident reflection coefficient of at least 40%. The best experimental results are obtained in the spectral range $\lambda = 13$–$18$ nm because mirrors have been synthesized[33,34] with the reflection coefficient exceeding 50%. The situation deteriorates at shorter wavelengths. For example, at $\lambda \approx 4.4$ nm the best reported reflection coefficient[35] of the mirrors intended for resonators in soft x-ray lasers is 12–15%, which is 4–5 times less than the maximum theoretical value. The greatest difficulties are encountered at even shorter wavelengths ($\lambda < 4.4$ nm), which are of special interest in x-ray lithography, because in this case the reflection coefficient of multilayer mirrors does not yet exceed a few percent (for near-normal incidence).

The selection of the pairs of materials for multilayer mirrors in the wavelength range $\lambda < 4.4$ nm is not so obvious as in the case of longer wavelengths ($\lambda > 4.4$ nm), where extensive use is made of mirrors containing carbon ($4.4 < \lambda < 12.4$ nm) and silicon ($\lambda > 12.4$ nm) as the weakly absorbing components. At wavelengths $2 < \lambda < 4$ nm these substances have high absorption coefficients, so that the calculated reflection coefficients of such mirrors are low: 10–30% (Fig. 7). The reflection coefficients of mirrors containing beryllium are approximately twice as high, but the technology of synthesis of multilayer structures containing Be is not sufficiently advanced.[36] Mirrors containing Ca, V, Sc, and Ti as the weakly absorbing components are described in Ref. 37. These materials have low absorption near the $L$ edges, which are located exactly in the wavelength range

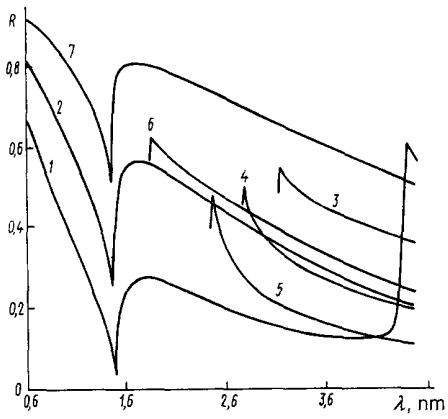


FIG. 7. Reflection coefficient of multilayer mirrors in which one component is Ni, determined for the short-wavelength soft x-ray range; the second component of the structure is: *1*) C; *2*) Be; *3*) Sc; *4*) Ti; *5*) V; *6*) LiF; *7*) LiH.

$\lambda \sim 2$–$4$ nm. In narrow spectral intervals the reflection coefficients of such structures can reach 40–60%.

The highest reflectivity is exhibited by the mirrors which contain substances with minimal absorption, such as LiH or LiF. For example, the reflection coefficients of an Ni–LiH structure exceed 50% throughout the wavelength range $\lambda < 4.4$ nm and reach 90% at $\lambda \approx 0.6$ nm. Such high reflection coefficients are providing a stimulus for the development of the technology of deposition of thin LiH and LiF films. However, no experiments have yet been carried out.

It should be stressed that the effectiveness of multilayer optics in the case of broadband soft x-ray sources is governed by the reflection coefficient $\int R(\lambda)/d\lambda$ integrated over the spectrum and not by its peak value. At shorter wavelengths the integral reflection coefficient falls strongly because of a reduction in the discontinuity of the permittivity at the interfaces between the media when the wavelength is reduced. For example, at $\lambda \approx 10$ nm the maximum integral reflection coefficient is about 0.2 nm, whereas at $\lambda \approx 5$ nm it is only 0.02 nm (Ref. 38).

The minimum period of multilayer coatings is governed by the technological feasibility of preparing continuous ultrathin films used in a structure and it is governed by the island growth of films evaporated by electron-beam or magnetron methods. Considerable progress has already been made. For example, it is reported in Ref. 39 that a multilayer W–$B_4C$ mirror with a period of about 0.7 nm was constructed. Record values were reported for Nb–Ti (period 0.6 nm) and PbSe–FeB (period 0.23 nm) structures.[40,41] It should be stressed that the latter structure was not intended for x-ray optics.

The main factor limiting the reflectivity of short-period mirrors is the roughness of the interfaces between layers. It follows from the Debye–Waller factor that the influence of such roughness on the reflection coefficient is weak provided the height of the irregularities does not exceed $\lambda/20$ (in the normal-incidence case).[42] This means that, for example, in the case of a mirror with a period 1.5 nm (reflecting normal incident $\lambda \approx 3$ nm radiation) the interface irregularities should be less than 0.15 nm in height, and if this height reaches 0.4 nm, the reflection coefficient falls by a factor of approximately 10. Island growth of films and interplanar

irregularities are responsible for the fact that at present one can speak of practical mirrors with the period $l \gtrsim 1.5$ nm, i.e., in the case of normal-incidence optics mirrors are available only for the soft x-ray range $\lambda > 3$ nm.

We cannot exclude that new opportunities for the fabrication of multilayer structures with ultrashort periods will be provided by the use of epitaxial methods of growth of crystal superlattices for the specific applications in soft x-ray optics. For example, experiments have shown that the period of EuS–PbS superlattices can be just 0.6 nm. This value is governed by the mismatch of the crystal lattices of the adjacent layers. Calculations show that near the $M$ absorption edge of Eu ($\lambda \approx 1.1$ nm) the reflection coefficient of such a multilayer structure can reach 20%.

Epitaxial superlattices are particularly interesting because of the fundamentally different film growth mechanism, which is atomic layer-by-layer and not of the island type. This is the reason why mirrors with an extremely low height of the interplanar irregularities may be prepared in this way, i.e., such mirrors should have fairly high experimental reflection coefficients, in spite of the far from optimal optical constants of the substances in an epitaxial structure. Naturally, final conclusions cannot be drawn about the potential use of such structures in soft x-ray optics without more careful theoretical and experimental investigations.

In addition to reducing the specular reflection coefficient, interface irregularities give rise to scattered radiation. This effect may be much more important in the case of multilayer normal-incidence objectives, which are proposed for projection x-ray lithography systems with submicron resolution. If the reduction in the specular reflection simply reduces the efficiency of an x-ray optical system, then the scattered radiation may limit the spatial resolution. In fact, the angular width of the scattering indicatrix is $\lambda/\pi a$ for normal incidence (here, $a$ is the correlation radius of the heights of the irregularities). Therefore, the size of the scattering spot on the surface of a resist is of the order of $\lambda F/\pi a$, where $F$ is the focal length of the objective. If the intensity of the scattered radiation is low, then this is the minimum spatial resolution. At $\lambda \sim 4$ nm, $a \sim 10\,\mu$m, and $F \sim 3$ cm, the best resolution is about 4 $\mu$m. Consequently, submicron resolution is attainable only if the intensity of the scattered radiation is low, i.e., if the height of the interface irregularities does not exceed a few tenths of a nanometer. The modern technology of superpolishing of substrates of complex shape and of synthesis of multilayer structures give hope that this requirement will be satisfied.

It therefore follows from consideration of multilayer x-ray optics that the longer the wavelength of the radiation used, the higher the efficiency of the x-ray optical systems and the lower the intensity of the radiation scattered by the interface irregularities.

It follows from modern ideas that the structure of interlayer interfaces, their quality, and stability are extremely important for time, thermal, and radiation stability of multilayer x-ray mirrors. Multilayer mirrors for the soft x-ray range, consisting of ultrathin layers of different materials, are as a rule nonequilibrium thermodynamic systems with a tendency for a gradual change in the optical characteristics with time. The instability of multilayer structures is particularly important at elevated temperatures and under the action of high radiation fluxes. For example, after annealing of

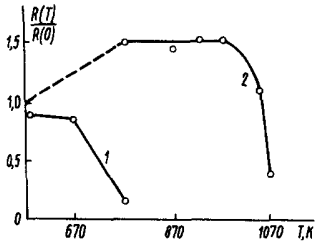


FIG. 8. Reflection of 20-period Mo–Si (*1*) and $MoSi_2$–Si (*2*) mirrors with a period of ~8 nm, plotted as a function of the annealing temperature $T$ (annealing period 1 h).

mirrors consisting of Mo–Si, W–Si, and W–C layer pairs at 600–700 K for 1–2 h, the reflection coefficients fall by a factor of 20–30, which implies a practically complete degradation of these mirrors (Fig. 8).

There is a whole range of mechanisms responsible for ageing of multilayer mirrors: sintering of planar layers because of the diffusion of atoms along the interfaces; diffusion mixing of neighboring layers forming liquid or solid solutions and compounds; deformation and cracking of multilayer coatings because of relaxation of stresses in the multilayer mirror–substrate system; there are also other mechanisms. We can avoid or at least weaken the destructive effects of such mechanisms by selecting the substances to be used in multilayer mirrors with the following points in mind. The pairs of materials should be in thermodynamic equilibrium at their interfaces, they should have the highest possible melting point, their thermal expansion coefficients should be equal, they should wet one another, they should not undergo phase structural or phase transitions under the influence of external agencies, etc. Finally, the optical constants of the materials should be such so as to ensure high reflection coefficients in the required range of wavelengths in the soft x-ray range. It is obvious that it is hardly possible to satisfy all these requirements simultaneously. In the selection one should therefore try to satisfy at least the most important of these.

Experiments have shown that the approach to a thermodynamic equilibrium at the interface between two materials can increase greatly the thermal stability of multilayer mirrors. We shall discuss this problem in greater detail by considering an Mo–Si mirror. A thermodynamic equilibrium at the interface between two phases is possible only if these phases are neighbors in the phase diagram of the binary system of alloys, i.e., if they are adjacent in the following series of molybdenum–silicon compounds: Mo, $Mo_3Si$, $Mo_5Si_3$, $MoSi_2$, Si. Therefore, a thermodynamic equilibrium between pure Mo and Si is impossible, because Mo adjoins the silicide $Mo_3Si$, and Si is next to the silicide $MoSi_2$. Moreover, formation of molybdenum silicides at the interfaces in an Mo–Si mirror is unavoidable.

The silicide $MoSi_2$ at the interfaces between the Mo and Si layers had indeed been discovered under an electron microscope after annealing of an Mo–Si mirror at 700 K or higher. Formation of molybdenum silicides increases considerably the irregularities of the interfaces and destroys almost completely the reflectivity of Mo–Si mirrors. The appearance of the silicide $MoSi_2$ facilitates such layer modification processes as migration of grains, dislocations,

and other defects in polycrystalline Mo films and also crystallization of amorphous Si films. Moreover, the specific volume of $MoSi_2$ is less than that of Mo and Si, so that the annealing reduces the period of an Mo–Si mirror by 18%.

It follows from this discussion that mixing of the adjacent layers (i.e., degradation of a multilayer structure) can be avoided if the pair $MoSi_2$ and Si is used instead of pure Mo and Si. The former materials ($MoSi_2$ and Si) are neighbors in the phase diagram and, consequently, the interface between them should be much more stable.

It is, in fact, found that the reflectivity of $MoSi_2$–Si mirrors falls only at temperatures exceeding 1000 K (Fig. 8). Moreover, contrary to the behavior of a multilayer Mo–Si structure, the reflection coefficient of an $MoSi_2$–Si mirror (at $\lambda = 0.154$ nm) increases by a factor of about 1.5 as a result of annealing at temperatures below 1000 K. In our opinion this is due to a reduction in the height of the interface irregularities. The use of annealing for smoothing out the interfaces may prove particularly useful in the synthesis of short-period structures. The change in the period of such an $MoSi_2$–Si mirror after annealing does not exceed a few percent. Degradation of the $MoSi_2$–Si structure at temperatures above 1000 K is due to crystallization of amorphous Si films, recrystallization of polycrystalline $MoSi_2$ films, and transformation of $MoSi_2$ from the hexagonal to the tetragonal structure. All these processes occur at high temperatures and cause sintering of the $MoSi_2$ and Si layers, i.e., they increased considerably the interface irregularities.

It follows that the much higher thermal stability of $MoSi_2$–Si mirrors compared with Mo–Si structures is the result of an approach to thermodynamic equilibrium at the interfaces between the two materials in each case. The maximum working temperature of $MoSi_2$–Si mirrors exceeds 1000 K, which is much higher than that of Mo–Si mirrors (up to 600 K).

Highly stable x-ray $MoSi_2$–Si mirrors may replace Mo–Si mirrors only if they have suitable optical characteristics. A comparison of the theoretical maximum reflection coefficient $R(\lambda)$ and of the effective number of periods $N_{\text{eff}}(\lambda) \sim \lambda/\Delta\lambda$ that contribute to the reflection by Mo–Si and $MoSi_2$–Si mirrors was carried out for wavelengths $\lambda > 12.4$ nm using expressions from Ref. 38. It is clear from Fig. 9 that in the range $\lambda > 15$–20 nm the $MoSi_2$–Si and Mo–Si mirrors have practically the same values of $R(\lambda)$ and $N_{\text{eff}}(\lambda)$. Only near a jump in the photoabsorption of silicon (at $\lambda \approx 12.4$ nm) do the Mo–Si mirrors exceed the $MoSi_2$–Si

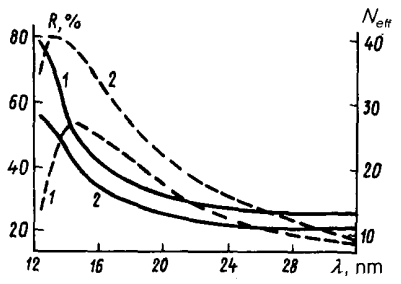


FIG. 9. Maximum attainable reflection coefficients for normal incidence in the long-wavelength part of the soft x-ray range (continuous curves) and effective number of periods contributing to reflection (dashed curves), obtained for Mo–Si (*1*) and $MoSi_2$–Si (*2*) mirrors.

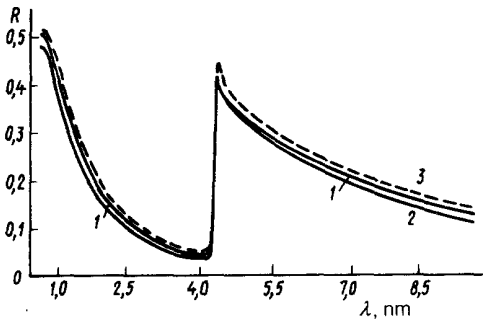


FIG. 10. Maximum attainable reflection coefficients for normal incidence of soft x-ray radiation on TaC–C (*1*) and HfC–C (*2*) multilayer mirrors. For comparison, the figure includes the $R(\lambda)$ curve for an Hf–C mirror (*3*), which was close to curve 2.

structures in reflectivity and the difference is 10–20%.

Experimental determination of the reflection coefficients of $MoSi_2$–Si and Mo–Si mirrors in the soft x-ray range had been made for the normal-incidence case by the method described in Ref. 43. The period of both mirrors was 7.5 nm and the number of periods was 40. The measured reflection coefficients were found to be 35% for an Mo–Si mirror (at $\lambda = 14.3$ nm) and 52% for an $MoSi_2$–Si mirror (at $\lambda = 14.5$ nm). This was evidence of much smoother interfaces in the case of the $MoSi_2$–Si structure. Annealing of the $MoSi_2$–Si mirror at 500 K for 1 h did not change the reflection coefficient.

It was thus found that the optical parameters of the $MoSi_2$–Si mirror satisfied the requirements for practical use in both respects: the value of the reflection coefficient and the thermal stability.

Similar results were reported for multilayer $WSi_1$–Si and WC–C mirrors when once again the material pairs were selected allowing for the requirement to approach a thermodynamic equilibrium at the interfaces between the layers. In our opinion, an even higher thermal stability can be expected of HfC–C and TaC–C structures. Moreover, these two pairs are not only in a thermodynamic equilibrium with one another, but also have very high melting points. The reflection coefficients calculated in the soft x-ray range for the HfC–C and TaC–C mirrors are shown in Fig. 10.

The selection of the pairs of materials for the synthesis of multilayer x-ray mirrors, based on the principle of attainment of a thermodynamic equilibrium at the interface between the media, makes it possible to increase considerably the thermal stability of the mirrors by reducing the destructive influence on a multilayer structure of such factors as the diffusion and formation of chemical compounds at the interfaces between the layers.

We can therefore assume that the radiation loads on multilayer x-ray optical components are not a serious obstacle to the development of projection x-ray lithography. Additional investigations may be needed in order to determine the time stability of multilayer mirrors, which is important if the x-ray optical components are to be made on a mass scale.

## 6. PROGRAM FOR NUMERICAL MODELING OF RAY PATHS IN SOFT X-RAY OPTICS

Calculation and analysis of the distortions contributed by different optical systems is one of the main tasks in geometric optics. It is a relatively simple task to estimate the

distortions caused by diffraction of radiation by finite numerical apertures, whereas calculations of geometric aberrations are difficult and time-consuming. This is true also of the optical systems for the soft x-ray range.

The low reflection coefficient of soft x-ray radiation often makes it necessary to use strongly nonparaxial systems and low grazing angles. The geometric aberrations can be reduced by employing systems with several reflecting surfaces of the Wolter, Baez, Schwarzschild, and other types. The tasks of altering the direction of synchrotron radiation and concentration of soft x rays can be performed effectively by rotatable x-ray mirrors utilizing the whispering gallery effect and involving a large number of reflections.

Time-consuming analytic calculations which are involved when dealing with such systems can be avoided and their dominant characteristics can be found simply and efficiently by relying on programs for numerical modeling of ray paths. An important circumstance in the x-ray range is that programs of this kind can be used to model the scattering of radiation by surface irregularities.

It should be pointed out that there are two approaches to the writing of programs for numerical modeling of ray paths. The first is the deterministic approach and it involves attribution to each ray of a specific amplitude, which changes as a result of passage through the optical system. The process of reflection together with a change in the direction of propagation of a ray includes also a change in the amplitude $W$: $W = WR(\theta)$, where $R(\theta)$ is the reflection coefficient at the point of incidence of the ray. The advantage of this approach is the simplicity of description and the absence of a statistical indeterminacy. However, the latter is also a shortcoming: the deterministic approach is unsuitable for the description of scattering of radiation by surface irregularities.

From the latter point of view a more promising and complete is the probabilistic approach: all the rays traveling in an optical system are assumed to have the same amplitude of unity and the "ray lifetime" is considered from the point of view of probability: the probability of the appearance ("birth") of a ray is considered at a given point of a source along a given direction, the probability of specular reflection or scattering is then analyzed, etc.

In the probabilistic approach the radiation from a source is modeled by a probability density function $p(x,y,z,\mathbf{a})$, where $x$, $y$, and $z$ are the coordinates of the point in a source from which a ray is emerging and $\mathbf{a}$ specifies the direction.

The reflection of a ray is described as follows. Let $R(\theta)$ be the reflection coefficient for a ray incident at an angle $\theta$ and $\xi_c$ be a random quantity distributed uniformly in the interval [0, 1] and found by a suitable random number generator for each reflection. The amplitude of a specularly reflected ray is then $W = 1$ for $R(\theta) \geqslant \xi_c$ and $W = 0$ for $R(\theta) < \xi_c$. The second case, when $W = 0$, corresponds to extinction ("death") of the ray. The use of the probability density function corresponding to a given scattering indicatrix $I(\theta,\varphi)$ makes it possible to describe the scattering of radiation on irregularities of the reflecting surface by the probability $p(\theta,\varphi) \propto I(\theta,\varphi)$.

The shortcomings of the probabilistic approach are the need to use a large number of rays to ensure an insignificant statistical error (because the relative error in the determination of the minimum element of an image is $\Delta n/n = n^{-1/2}$, where $n$ is the number of rays defining this element) and the difficulties encountered in the determination of the necessary probability density functions. A file of programs, written and tested at the Lebedev Physics Institute, is based on this probabilistic approach. We shall now consider the use of these programs in greater detail.

A radiation source is represented by a thin disk or a geometric point emitting isotropically forward half-space. The programs allow for the possibility of an off-axial position of a source and also for the matching of the angle of emission from the source to the entry aperture of an optical system in order to increase the efficiencyof illumination. A shift of a point source makes it possible to analyze the resolution in the object field and, in the case of a source of finite dimensions, to obtain real characteristics of its image.

In this file of programs the reflection is modeled ignoring the scattering, but a real reflection coefficient is found using the Fresnel formulas. The direction vector $\mathbf{a}$ of the reflected ray is found from $\mathbf{a} = \mathbf{a}_0 + 2(\mathbf{a}_0,\mathbf{n})$, where $\mathbf{a}_0$ is the direction vector of the incident ray and $\mathbf{n}$ is a unit internal normal to the surface at the point of incidence of the ray. The presence of shadow and open stops is allowed for in these programs.

A wide range of problems can be tackled when the results of the numerical modeling of ray paths are outputted using four different methods.

1. In the first method the plane of a screen or a target is split into a rectangular network of cells. The program gives the number of rays $n(x,y)$ reaching each cell. The function $n(x,y)$ obtained in this way represents the distribution of the radiation flux over the screen area and it is then displayed as a surface (Fig. 11) or used in tables.

2. In the second method the points of intersection of rays with the plane of a screen are determined. A set of such points makes it possible to judge visually the distribution of the flux density (Fig. 12). This is particularly convenient by

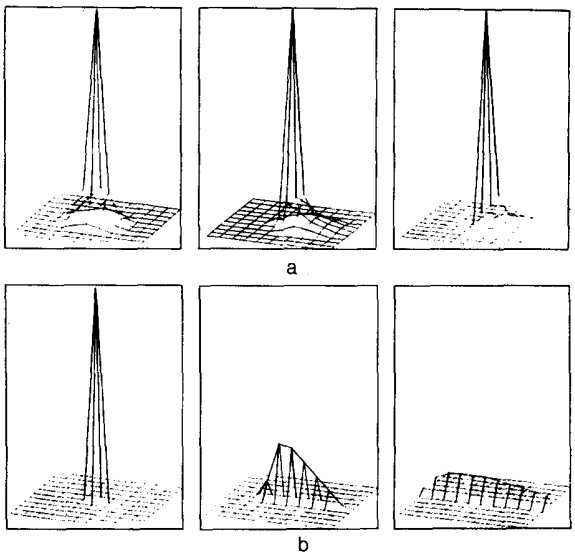


FIG. 11. Distribution of the flux density over the area of a target: the image of a point source is formed by a stopped-down spherical mirror at different displacements of the source from the optic axis in the case of smaller ($a$) and larger ($b$) diameters of the stop.

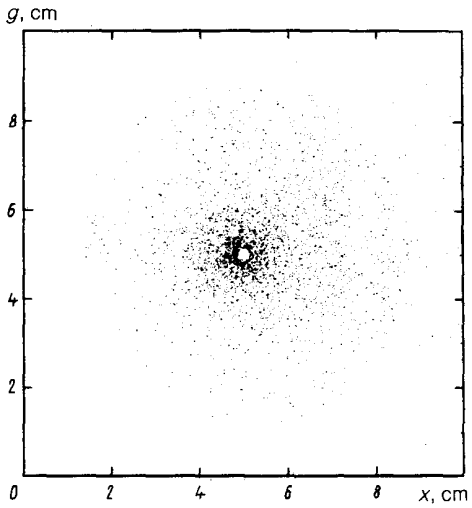


FIG. 12. Positions of rays in the target plane.

way of illustration and in a qualitative estimate of the results.

3. In this case the projections of rays are imaged graphically on an $XZ$ or $YZ$ plane (Fig. 13), which reveals conveniently the characteristics of the caustic and makes it possible to determine more accurately the position of the image plane.

4. In the fourth method, suitable for axisymmetric systems, the dependence of the flux density $q(r)$ on the distance $r$ from the center of a screen (axis of the system) is plotted as shown in Fig. 14, which makes it possible to reduce the statistical error.

This file of programs was used specifically to determine and analyze the resolution and the caustics of x-ray optical systems for projection lithography (Figs. 11 and 13) and the homogeneity of illumination of a sample using collimating x-

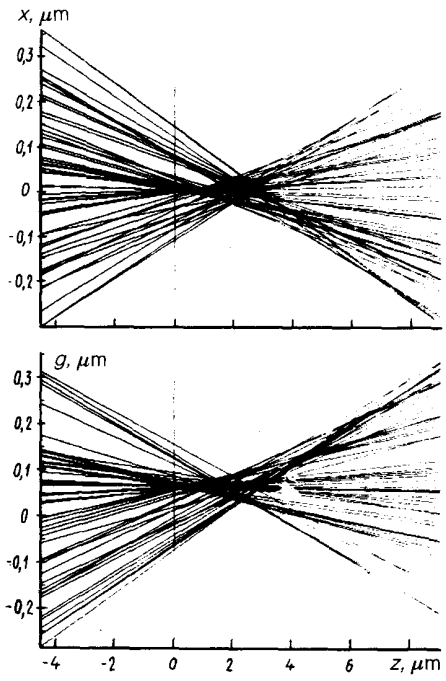


FIG. 13. Ray paths near the target plane.

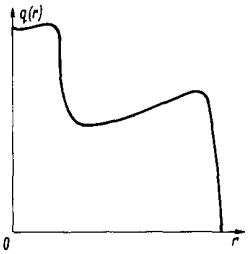


FIG. 14. Radiation flux density $q(r)$ on a target plotted as a function of the distance.

ray concentrators (Figs. 12 and 14). This made it possible to investigate the properties of a large class of optical systems: paraxial and experimental optics, grazing-incidence mirror systems with one or several reflections, rotatable mirrors utilizing the whispering gallery effect, etc., with any number of optical components.

Further developments of this file of programs may occur along the following directions: 1) the main advantage of the programs for numerical modeling of ray paths—which is the ability to describe relatively simply the operation of optical systems—makes them suitable for numerical experiments which should yield direct images of complex objects and facilitate the optimization of the experimental conditions; 2) the use of the probabilistic description makes it possible to allow for the influence of the scattering of radiation by irregularities of the reflecting surfaces on the imaging and concentration performed by x-ray optical systems.

## CONCLUSIONS

Optics has enriched x-ray lithography with two new possibilities: lithography with reduction by x-ray optical systems and lithography utilizing reflecting templates. The foremost task in the design of efficient systems and apparatus for projection x-ray submicron lithography is the construction of high-quality x-ray optical components and objectives. The long-term stability of mirrors against the effects of a plasma and x rays has not yet been investigated sufficiently thoroughly and will present a problem in future. In addition, the potential industrial use of projection x-ray lithography equipment will depend on such factors as the productivity, reliability, and service life of an x-ray source. Nevertheless, the development of x-ray optics and improvements in the technology of fabrication of x-ray mirrors open up new vistas of extensive use of point sources in x-ray lithography.

[1)] Laser Applications and Information Centre, Amsterdam, Nieuwegein, Netherlands.
[2)] V. I. Lenin Polytechnic Institute, Kharkov.
[3)] Scientific-Research Institute of Molecular Electronics, Zelenograd.

[1] W. C. Hittinger, Sci. Am. No. 8, 48 (August 1973).
[2] R. Noyce, Sci. Am. No. 9, 62 (September 1977).
[3] W. Moro, *Microlithography: Principles, Methods, Materials* [Russian translation], Mir, Moscow (1990).
[4] R. W. Hill, J. Vac. Sci. Technol. B **7**, 1387 (1989).
[5] M. Nisenoff, Cryogenics **28**, 47 (1988).
[6] R. Singh and B. A. Biegel, *Proc. Intern. Conf. on Thin Film Processing and Characterization of High-Temperature Superconductors*, Anaheim, CA, 1987 (ed. by J. M. E. Harper, R. J. Colton, and L. C. Feldman), in AIP Conf. Proc. No. 165, 211 (1988).
[7] M. Bolsen, G. Buhrr, H. Merren, and K. Van Werden, Solid State Technol. **29**(2), 87 (1986).
[8] Microelectron. Manuf. No. 12, 9 (1984).
[9] A. Jackson, Synchrotron Radiat. News **3**(3), 13 (1990).

[10] J. Warlaumont, J. Vac. Sci. Technol. B 7, 1634 (1989).
[11] G. P. Williams, Synchrotron Radiat. News 1(2), 21 (1988).
[12] Microelectron. Manuf. Test. No. 6, 7 (1988).
[13] Radioelektron. za Rubezhom No. 12, 5 (1989).
[14] Lambda Highlights No. 27-28, 4 (1991).
[15] H. Izawa, Denshi Tsire (Special Issue) **26**, 92 (1987).
[16] Semicond. Intern. No. 2, 49 (1987).
[17] Proc. IEE **17**, 46 (1987).
[18] N. Amoda, Denshi Tsire **21**, 134 (1982).
[19] E. Spiller, D. E. Eastman, R. Feder, W. D. Grobman, W. Gudat, and J. Topalian, J. Appl. Phys. **47**, 5450 (1976).
[20] K. A. Valiev, *Physics of Submicron Lithography* [in Russian], Nauka, Moscow (1990).
[21] A. V. Vinogradov, I. V. Kozhevnikov, and O. I. Tolstikhin, Kvantovaya Elektron. (Moscow) **14**, 1501 (1987) [Sov. J. Quantum Electron. **17**, 953 (1987)].
[22] A. V. Vinogradov and O. I. Tolstikhin, Tr. Fiz. Inst. Akad. Nauk SSSR **196**, 168 (1987).
[23] J. F. Young, J. J. Macklin, and S. E. Harris, Opt. Lett. **12**, 90 (1987).
[24] *Mirror X-Ray Optics* [in Russian], Mashinostroenie, Leningrad (1989).
[25] M. H. Muendel and P. L. Hagelstein, Proc. SPIE Int. Soc. Opt. Eng. **1229**, 87 (1990).
[26] A. V. Vinogradov, V. M. Elinson, V. I. Zhilina, N. N. Zorev, G. F. Ivanovsky, I. V. Kozhevnikov, M. E. Plotkin, S. I. Sagitov, V. A. Slemzin, and V. V. Sleptsov, Nucl. Instrum. Methods Phys. Res. A **261**, 101 (1987).
[27] A. V. Vinogradov, V. M. Elinson, I. V. Kozhevnikov, E. P. Savinov, S. I. Sagitov, and V. V. Sleptsov, Opt. Spektrosk. **67**, 206 (1989) [Opt. Spectrosc. (USSR) **67**, 117 (1989)].
[28] I. A. Artyukov, A. V. Vinogradov, and I. V. Kozhevnikov, Preprint No. 129 [in Russian], Lebedev Physics Institute, Academy of Sciences of the USSR, Moscow (1990).
[29] W. T. Welford and R. Winston, *The Optics of Nonimaging Concentrators: Light and Solar Energy*, Academic, New York (1978).
[30] N. N. Zorev, Tr. Fiz. Inst. Akad. Nauk SSSR **196**, 129 (1989).
[31] H. Kinoshita, K. Kurihara, Y. Ishii, and Y. Torii, J. Vac. Sci. Technol. B **7**, 1648 (1989).
[32] A. M. Hawryluk and L. G. Seppala, J. Vac. Sci. Technol. B **6**, 2162 (1988).
[33] T. W. Barbee Jr., S. Mrowka, and M. C. Hettrick, Appl. Opt. **24**, 883 (1985).
[34] V. V. Kondratenko, Yu. P. Pershin, O. L. Poltzeva, A. I. Fedorenko, E. N. Zubarev, S. A. Yulin, I. V. Kozhevnikov, S. I. Sagitov, V. A. Chirkov, V. E. Levashov, and A. V. Vinogradov, *Paper Presented at Intern. Conf. on Short Wavelength Lasers*, Samarkand, USSR, 1990.
[35] J. H. Underwood, *Paper Presented at Second Intern. Colloquium on X-Ray Lasers*, York, England, 1990.
[36] A. V. Vinogradov, I. V. Kozhevnikov, V. V. Kondratenko, I. I. Lyakhovskaya, A. T. Ponomarenko, S. I. Sagitov, and A. I. Fedorenko, Pis'ma Zh. Tekh. Fiz. **13**, 129 (1987) [Sov. Tech. Phys. Lett. **13**, 53 (1987)].
[37] A. D. Akhsakhalyan, S. V. Gaponov, S. A. Gusev, Yu. Ya. Platonov, N. N. Salashchenko, and N. I. Polushkin, Nucl. Instrum. Methods Phys. Res. A **261**, 75 (1987).
[38] I. V. Kozhevnikov and A. V. Vinogradov, Phys. Scri. T **17**, 137 (1987).
[39] A. F. Jankowski, D. M. Makowiecki, M. A. Wall, and M. A. McKernan, J. Appl. Phys. **65**, 4450 (1989).
[40] Y. J. Qian, J. Q. Zheng, B. K. Sarma, H. Q. Yang, J. B. Ketterson, and J. E. Hilliard, J. Low Temp. Phys. **49**, 279 (1982).
[41] A. L. Greer, in *Modulated Structure Materials*, Nijhoff, Dordrecht, Netherlands (1983), p. 491.
[42] J. M. Elson, J. P. Rahn, and J. M. Bennett, Appl. Opt. **22**, 3207 (1983).
[43] S. S. Borisova, I. V. Kozhevnikov, V. V. Kondratenko, V. E. Levashov, I. I. Lyakhovskaya, I. F. Mikhaĭlov, A. G. Ponomarenko, S. I. Sagitov, A. I. Fedorenko, V. A. Chirkov, and A. S. Shulakov, Zh. Tekh. Fiz. **59**(3), 78 (1989) [Sov. Phys. Tech. Phys. **34**, 298 (1989)].

Translated by A. Tybulewicz